

Systems Science & Control Engineering

An Open Access Journal

ISSN: (Print) (Online) Journal homepage: <https://www.tandfonline.com/loi/tssc20>

Mixed sensitivity control: a non-iterative approach

R. Galindo Orozco

To cite this article: R. Galindo Orozco (2020) Mixed sensitivity control: a non-iterative approach, Systems Science & Control Engineering, 8:1, 441-453, DOI: [10.1080/21642583.2020.1793821](https://doi.org/10.1080/21642583.2020.1793821)

To link to this article: <https://doi.org/10.1080/21642583.2020.1793821>



© 2020 The Author(s). Published by Informa UK Limited, trading as Taylor & Francis Group.



Published online: 23 Jul 2020.



Submit your article to this journal [↗](#)




View related articles [↗](#)



View Crossmark data [↗](#)

Mixed sensitivity control: a non-iterative approach

R. Galindo Orozco 

Faculty of Electrical and Mechanical Engineering, Autonomous University of Nuevo Leon, San Nicolas de los Garza, Mexico

ABSTRACT

Recent analytical solutions to Mixed Sensitivity Control (MSC) are developed and compared with standard MSC based on γ -iteration. The proposed MSC solution gives conditions for strong stability and overcomes the pole-zero cancellations between the plant and the controller of non-iterative solutions, keeping the low-computational effort advantage of non-iterative solutions. The proposed MSC is based on the minimization of the most common closed-loop sensitivity functions in low-frequencies and the free-parameters of the stabilizing-controllers solve an algebraic equation of restriction that assigns the same value to the infinity-norms of the sensitivity functions at low and high-frequencies, guaranteeing robust stability and robust performance. It is assumed that the plant state dimension is double the plant input dimension and that the linear time-invariant nominal plant has a stabilizable and detectable realization and is strongly stabilizable. This MSC problem is solved in a one-parameter observer-controller configuration and reference tracking-control of positions is realized on a two-degrees of freedom feedback-configuration. An approximated optimal value of the location of the closed-loop poles is proposed based on Glover and McFarlane's optimal stability margin [(1989)] which in turn is based on Nehari's Theorem. Simulations of a mechanical system illustrate the results.

ARTICLE HISTORY

Received 17 January 2020
Accepted 6 July 2020

KEYWORDS

Robust control; robust stability; robust performance; mixed sensitivity; stabilizing controllers; unstructured uncertainty; sub-optimal control; γ -iteration

1. Introduction

Robust \mathcal{H}_∞ control (see for instance the book of Zhou et al. (1996)) has been successfully applied to the optimal control, analysis and design of systems subject to disturbance and unstructured uncertainties, like unmodelled dynamics. There is no information for these type of uncertainties except that an upper bound on its \mathcal{H}_∞ norm as a function of frequency. Closed-loop stability under uncertainties is guaranteed by the Small Gain Theorem.

One useful robust control technique is Mixed Sensitivity Control (MSC) that reduces closed-loop sensitivity to \mathcal{H}_2 norm bounded disturbances and \mathcal{H}_∞ norm bounded uncertainties. A data-driven approach of MSC is proposed by Fomentin and Karimi (2013) and is applied to an active suspension system. The present work focus on model-based design. There are two general approaches to solve the MSC problem, both based on the solution of two-Riccati equations: the non-iterative approach proposed by Glover and McFarlane (1989) and the γ -iteration approach proposed by Doyle et al. (1989). The non-iterative solution generally suffers from pole-zero cancellations between the plant and the controller and heavily depends on the selection of weighting functions (see Tsai et al., 1992). It is pointed out that pole-zero cancellation is dependent upon the choice of weighting functions and

the particular construction of weighting function is given to prevent the phenomenon. Two techniques are compared in the work of Folly (2007) that prevent pole-zero cancellation of the Riccati-based MSC approach. On the other hand, the sub-optimal solution of the γ -iteration approach has been further developed using Linear Matrix Inequalities (LMI) that provide more flexibility for combining various design objectives.

Recent applications of MSC based on γ -iteration are the works of Banerjee et al. (2018), Ounis and Golea (2016), Diaz et al. (2015) and Cerone et al. (2009). In the work of Banerjee et al. (2018) to damp inter-area oscillations of grids, a multiterminal DC-current injection is modelled as disturbances using an MSC formulation in the LMI framework, in the work of Ounis and Golea (2016) to address the DC-DC Buck converter control, sensitivity functions are used to specify the desired design requirements and γ -iteration is used to tune Proportional Integral Derivative (PID) control parameters, in the work of Diaz et al. (2015) a Linear Parametric Varying (LPV) controller applied to a wind turbine, is based on the solution of LMI's proposed in an MSC scenario, and in the work of Cerone et al. (2009), an MSC of the yaw movement of a vehicle is realized in a two-degrees of freedom (*d.o.f.*) feedback configuration and is implemented on

CONTACT R. Galindo Orozco  rgalindoro@gmail.com, rene.galindoorz@uanl.edu.mx

a hardware-in-the-loop simulation. Also, recent applications based on the non-iterative approach are the works of Sutiyasadi and Parnichkun (2016) and Sil et al. (2009). In the work of Sutiyasadi and Parnichkun (2016) to overcome the uncertainties and disturbances, an MSC was proposed to control a quadruped robot legs positions, and a power system stabilizer is designed by Sil et al. (2009), using weighted MSC.

The present work overcomes the pole-zero cancellations between the plant and the controller of non-iterative solutions, keeping the advantages of analytical solutions such as low computational effort that is useful for on-line control implementation.

Usually, the plant input and output disturbances are attenuated at the plant output in low-frequencies while the disturbance at the measurement and the stable unstructured uncertainties are attenuated at the plant output in high-frequencies. So, the feedback configuration satisfies the compromises between the disturbance and uncertainties sensitivity reduction in the frequency bandwidths in which the disturbance and uncertainties are more significant. In this approach are the works of Galindo and Flores (2014), Galindo and Conejo (2012) and Galindo (2009). In the work of Galindo and Flores (2014), MSC is synthesized for each vertex of the convex hull of the plant, and an LPV controller is designed by interpolation of these robust controllers.

For systems satisfying the assumptions of Section 2, the contributions of this paper are,

- (1) Recent results on MSC proposed in the works of Galindo and Conejo (2012) and Galindo (2009) are further developed in a one-parameter observer-controller configuration in Section 3 for the criterion,

$$\inf_{K(s)} \left\| \begin{bmatrix} S_o(s) & S_o(s)P(s) \\ K(s)S_o(s) & T_i(s) \end{bmatrix} \right\|_{\infty} \quad (1)$$

that is also used in the work on MSC of Glover and McFarlane (1989), where $S_o(s) := (I + P(s)K(s))^{-1}$ is the output sensitivity function, $P(s)$ is the nominal plant, $K(s)$ is the stabilizing controller and $T_i(s) := K(s)S_o(s)P(s)$ is the complementary input sensitivity function.

- (2) Analytical expressions for the free parameters of the stabilizing controllers solving an MSC problem are established, i.e. the criterion (1) is minimized by decreasing $\| [S_o(s) \ S_o(s)P(s)] \|_{\infty}$ at low-frequencies subject to the algebraic equation of restriction that assigns the same value to this norm and $\| [K(s)S_o(s) \ T_i(s)] \|_{\infty}$ at high-frequencies. Moreover, it is shown that the proposed solution to the MSC problem, implies strong stability, that is, the stabilizing controllers are stable.

- (3) An approximated optimal value of the location of the closed-loop poles is proposed in Section 3, based on the optimal stability margin proposed by Glover and McFarlane (1989).
- (4) The stabilizing controller solving the MSC is used in a two-degrees of freedom (*d.o.f.*) feedback configuration where the reference controller assures reference tracking control of positions in Section 4.

The criterion (1) includes some of the most common transfer functions. Under \mathcal{H}_2 norm bounded inputs, the \mathcal{H}_2 norm of the outputs are related to the \mathcal{H}_{∞} norm of the associated transfer functions by Parseval's Lemma. The minimization of the criterion can be realized if $K(s)$ stabilizes $P(s)$, using the parametrization of all stabilizing controllers, the problem is transformed into an optimization problem without restrictions affine to the free control parameter (see the book of Vidyasagar (1985)). This fact was exploited in the works of Galindo and Conejo (2012) and Galindo (2009), and Section 3. The organization of the proposed results is depicted in Figure 1.

Notation: $\mathfrak{R}(s)$ denotes the set of all rational functions of the complex variable s with real coefficients; \mathfrak{RH}_{∞} the set of proper stable rational functions; \mathfrak{R} the set of real numbers; $A_l := \lim_{s \rightarrow 0} A(s)$ and $A_h := \lim_{s \rightarrow \infty} A(s)$ are the asymptotic approximations of a matrix $A(s) \in \mathfrak{R}(s)$, in low and high frequencies, respectively; and I_p the identity matrix of dimension p by p .

2. Problem statement

A one-parameter observer-controller configuration is shown in Figure 2, where $P(s) = H(sI_n - F)^{-1}G + J \in \mathfrak{R}^{p \times m}(s)$; $K(s) \in \mathfrak{R}^{m \times n}(s)$ and $K_o(s) \in \mathfrak{R}^{m \times n}(s)$ are the controllers; $v(t) \in \mathfrak{R}^m$ and $y_m(t) \in \mathfrak{R}^p$ are $P(s)$ input and output measurement, respectively; $x_d(t) \in \mathfrak{R}^n$ is the state input reference; T_1 and T_2 are linear similarity transformations, and $d_o(t) \in \mathfrak{R}^p$ and $d_m(t) \in \mathfrak{R}^p$ are external disturbances at the output and the measurement of $P(s)$, respectively. The estimated state $\hat{x}(t) \in \mathfrak{R}^n$ is generated at the bottom of Figure 2 and the estimated error $x_d - \hat{x}(t)$ is used by the one-parameter controller $K(s)$ that stabilizes $P(s)$.

In the present work, it is assumed that,

- A1 MIMO, causal, proper, lumped, and LTI nominal plants having stabilizable and detectable realizations, are considered. In what follows the controllable and observable subsystem is considered as a given nominal plant $P(s)$, that is assumed to be square.
- A2 As in the works of Galindo (2016), Galindo and Conejo (2012) and Galindo (2009), the state dimension of

MatLab function `hinfsyn`. This state-space approach was proposed by Doyle et al. (1989) where the stabilizing controller exists if and only if two algebraic Riccati equations are positive definite.

Remark 2.1: In the circle model for unstructured uncertainties, $\Delta(s)$, i.e. $\|\Delta(s)\|_\infty \leq m$, where $m \in \mathfrak{R}$, the worst case of uncertainties happens at high frequencies (see Zhou et al., 1996). So, the Small Gain Theorem assures robust stability if, $\|T_{u_{\Delta}y_{\Delta}}(s)\|_\infty \leq 1/m$ at high frequencies, where $T_{u_{\Delta}y_{\Delta}}(s)$ is the transfer function from the output of $\Delta(s)$, $y_{\Delta}(t)$, to the input of $\Delta(s)$, $u_{\Delta}(t)$. Since $T_{u_{\Delta}y_{\Delta}}(s)$ is $K(s)S_o(s)$ and $T_i(s)$ for additive and input multiplicative uncertainty models, respectively, then robust stability is assured when solving Problem 2.1 if,

$$\|G_h\|_\infty \leq \frac{1}{m} \quad (5)$$

when both additive and input multiplicative uncertainty models are expected. If only additive uncertainty models are expected then robust stability is guaranteed if $\|K_h S_{oh}\|_\infty \leq 1/m$ while this condition for multiplicative uncertainty models is $\|T_{ih}\|_\infty \leq 1/m$.

In the work of Galindo (2016) the results of Galindo and Conejo (2012) and Galindo (2009) have been extended to proper $P(s)$, in the feedback configuration of Figure 2, where J is cancelled by the observer into the dynamic equation of the estimation error, and the dynamic state equation of $P(s)$ does not depend on J , so, without loss of generality, the strictly proper part (F, G, H) of the realization of $P(s)$ is considered, to design the stabilizing controllers. However, the transfer function from $x_d(s)$ to $y_m(t)$ is a function of J and has been taken into account for the I/O decoupling problem in the work of Galindo (2016). The controller is designed in new coordinates under the change of basis $\chi(t) := T_1 x(t)$ and $\eta(t) := T_2 x(t)$, in the feedback configuration of Figure 2. Then, as in Galindo and Conejo (2012), the separation principle is applied to split the problem, i.e. the controller is designed for a realization (A, B, I_n) , and the observer is designed for a realization (A_o, I_n, C_o) , in new coordinates, and are implemented in the feedback configuration of Figure 2. The mistake in the rows order of T_2 of the work of Galindo and Conejo (2012) was amended in the work of Galindo (2016) and the correct T_2 is used in the present work.

In the work of Galindo and Conejo (2012), the change of basis $\chi(t) := T_1 x(t)$ and $\eta(t) := T_2 x(t)$ have been used, where,

$$T_1 = \begin{bmatrix} I_m & -G_1 G_2^{-1} \\ V_1 \Theta_1 & I_m \end{bmatrix} \quad (6)$$

and

$$T_2 = \begin{bmatrix} \Delta_2^{-1} & -\Delta_2^{-1} \Theta_2 V_2 \\ H_2^{-1} H_1 \Delta_2^{-1} & I_m - H_2^{-1} H_1 \Delta_2^{-1} \Theta_2 V_2 \end{bmatrix} \quad (7)$$

being $V_1 := (F_{12} - G_1 G_2^{-1} F_{22})^{-1}$, $\Theta_1 := F_{11} - G_1 G_2^{-1} F_{21}$, $\Delta_1 := I_m + G_1 G_2^{-1} V_1 \Theta_1$, $V_2 := (F_{21} - F_{22} H_2^{-1} H_1)^{-1}$, $\Theta_2 := F_{11} - F_{12} H_2^{-1} H_1$ and $\Delta_2 := I_m + \Theta_2 V_2 H_2^{-1} H_1$, are given to obtain,

$$A = \begin{bmatrix} 0 & A_{12} \\ A_{21} & A_{22} \end{bmatrix}, \quad B = \begin{bmatrix} 0 \\ B_m \end{bmatrix}, \quad C = [C_1 \quad C_2] \quad (8)$$

and

$$A_o = \begin{bmatrix} 0 & A_{12o} \\ A_{21o} & A_{22o} \end{bmatrix}, \quad B_o = \begin{bmatrix} B_1 \\ B_2 \end{bmatrix}, \quad C_o = [0 \quad C_m] \quad (9)$$

that are special structures of the realization of $P(s)$ for the controller and observer designs, respectively when the separation principle is applied.

Analytical solutions of right and left coprime factorizations (*r.c.f.* and *l.c.f.*, respectively) over \mathfrak{RH}_∞ of $(sI_n - A)^{-1}B = N(s)D^{-1}(s) = \tilde{D}^{-1}(s)\tilde{N}(s)$ and $C_o(sI_n - A_o)^{-1} = N_o(s)D_o^{-1}(s) = \tilde{D}_o^{-1}(s)\tilde{N}_o(s)$, respectively, and solutions to the Diophantine equations $X(s)N(s) + Y(s)D(s) = I$ and $\tilde{N}_o(s)\tilde{X}_o(s) + \tilde{D}_o(s)\tilde{Y}_o(s) = I$, are given in Appendix that have been proposed in the works of Galindo (2016) and Galindo and Conejo (2012), in which $\tilde{N}(s)$ and $N(s)$ are of first-order rather than the ones of second-order proposed in the work of Galindo and Conejo (2012). Then, $K(s)$ and $K_o(s)$ in the feedback configuration of Figure 2 belong to the set of all controllers that stabilize $(sI_n - A)^{-1}B$ and $C_o(sI_n - A_o)^{-1}$, respectively, and the reference controller $K_r(s)$ are given by the parametrization of all stabilizing controllers (see Vidyasagar, 1985),

$$\begin{aligned} K(s) &= \tilde{D}_k^{-1}(s)\tilde{N}_k(s), \\ K_o(s) &= N_{ko}(s)D_{ko}^{-1}(s) \quad \text{and} \\ K_r(s) &= \tilde{D}_k^{-1}(s)Q(s) \end{aligned} \quad (10)$$

where $\tilde{D}_k(s) = Y(s) - R(s)\tilde{N}(s)$, $\tilde{N}_k(s) = X(s) + R(s)\tilde{D}(s)$, $N_{ko}(s) := \tilde{X}_o(s) + D_o(s)\tilde{R}(s)$ and $D_{ko}(s) := \tilde{Y}_o(s) - N_o(s)\tilde{R}(s)$, being $R(s) = [R_1(s) \quad R_2(s)] \in \mathfrak{RH}_\infty^{m \times n}$, $Q(s) \in \mathfrak{RH}_\infty^{m \times n}$ and $\tilde{R}(s) = [\tilde{R}_1^T(s) \quad \tilde{R}_2^T(s)]^T \in \mathfrak{RH}_\infty^{m \times n}$ free control parameters, satisfying $\det(\tilde{D}_k(s)) \neq 0, \forall s$ and $\det(D_{ko}(s)) \neq 0, \forall s$. It is shown in Vidyasagar (1985) that 'almost all' $R(s)$ and $\tilde{R}(s)$ satisfy $\det(\tilde{D}_k(s)) \neq 0, \forall s$ and $\det(D_{ko}(s)) \neq 0, \forall s$.

On the other hand, in the work of Glover and McFarlane (1989), a normalized left coprime factorization (*n.l.c.f.*) of $P(s) = \tilde{D}^{-1}(s)\tilde{N}(s)$ is used and is given by,

Lemma 2.1: Let $P(s) = C(sI - A)^{-1}B + E$ with (A, B, C, E) be a minimal realization. Then, a *n.l.c.f.* of $P(s)$, $\tilde{D}^{-1}(s)\tilde{N}(s)$

is,

$$\begin{aligned}\tilde{N}(s) &= R^{-1/2}C(sI - A - HC)^{-1}(B + HE) + R^{-1/2}E \\ \tilde{D}(s) &= R^{-1/2}C(sI - A - HC)^{-1}H + R^{-1/2}\end{aligned}\quad (11)$$

where $R := I + EE^*$ and $H := -(ZC^* + BE^*)R^{-1}$ being $Z > 0$ the unique solution of the Generalized Filter Algebraic Riccati Equation (GFARE),

$$A_f Z + Z A_f^* - Z C^* R^{-1} C Z + B(I - E^* R^{-1} E)^{-1} B^* = 0 \quad (12)$$

where $A_f := A - BE^* R^{-1} C$.

In the above Lemma, $\tilde{D}(s)$ is square, $\det(\tilde{D}(s)) \neq 0$, $\exists \tilde{X}(s) \in \mathfrak{RH}_\infty$ and $\tilde{Y}(s) \in \mathfrak{RH}_\infty$ such that $\tilde{N}(s)\tilde{X}(s) + \tilde{D}(s)\tilde{Y}(s) = I$ and $\tilde{N}(s)\tilde{N}^*(s) + \tilde{D}(s)\tilde{D}^*(s) = I$. This factorization is equivalent to $[\tilde{N}(s) \ \tilde{D}(s)]$ be co-inner, preserving the \mathcal{H}_∞ norm. For *n.l.c.f.*, the criterion given by Equation (1) is equivalent to,

$$\inf_{K(s)} \left\| \begin{bmatrix} I \\ K(s) \end{bmatrix} S_o(s) \tilde{D}^{-1}(s) \right\|_\infty \quad (13)$$

This problem fits into the standard \mathcal{H}_∞ framework and can be solved using the standard iterative procedures. An advantage of electing the *n.l.c.f.* of Lema 2.1 is that the problem can be solved exactly and that the computationally expensive iterative procedure can be avoided.

Let (A, B, C, E) be a stabilizable and detectable realization of $P(s)$, and $X_r \geq 0$ and $Z \geq 0$ be unique solutions of the GFARE and of the Generalized Control Algebraic Riccati Equation (GCARE), respectively, where the GCARE is given by,

$$X_r A_k + A_k^* X_r - X_r B S^{-1} B^* X_r + C^* (I - E S^{-1} E^*) C = 0 \quad (14)$$

being $A_k := A - B S^{-1} E^* C$ and $S := I + E^* E$. Then, the minimal value γ^* of the criterion (13) is given by Glover and McFarlane (1989), where the proof is developed,

$$\gamma^* = \frac{1}{\epsilon_{\max}} = \sqrt{1 + \lambda_{\max}(Z X_r)} \quad (15)$$

This value is useful to compare suboptimal solutions, $\epsilon_{\max} = \sqrt{1 - \|\tilde{D}(s) \tilde{N}(s)\|_H^2}$ is the stability margin, where $\|\cdot\|_H$ is Hankel norm. In the work of Glover and McFarlane (1989) it is proved that the robust stability problem of Equation (13) is reduced to a Nehari extension problem based on co-inner matrices that preserves the \mathcal{H}_∞ norm. Then, ϵ_{\max} is gotten by Nehari's Theorem, that is, the Hankel norm is solved, assuring that the nearest unstable system to the stable nominal plant of the Nehari extension.

For a given value of $\gamma \geq \gamma^*$, a solution of an MSC problem was proposed by Glover and McFarlane (1989)

in state space. However, this solution generally produces undesired pole-zero cancellations between the plant and the controller and heavily depends on the election of weighting functions.

In the next section, a solution to Problem 2.1 is given.

3. Mixed sensitivity

First, asymptotic approximations of $S_o(s)$ and $S_o(s)P(s)$ at low frequencies, and of $K(s)S_o(s)$ and $T_i(s)$ at high frequencies, are proposed by,

Lemma 3.1: Consider the plants $(sI_n - A)^{-1}B$ and $C_o(sI_n - A_o)^{-1}$ where A and B are given by Equation (8), A_o and C_o are given by Equation (9), the left and right coprime factorizations of these plants and the solutions of the Diophantine equations are given in Appendix. Let $R(s)$ be $[R_1 \ R_2] \in \mathfrak{RH}_\infty^{m \times n}$ and $\tilde{R}(s)$ be $[\tilde{R}_1^T \ \tilde{R}_2^T]^T \in \mathfrak{RH}_\infty^{m \times n}$ and suppose that $K(s)$ and $K_o(s)$ are given by Equation (10) and that A_{21} and A_{21o} are non-singular matrices. Then, for $(sI_n - A)^{-1}B$,

$$\begin{aligned}S_{ol} &= \begin{bmatrix} \frac{1}{a^2} A_{12} \left(\frac{1}{a} R_2 - I_m \right) A_{21} \\ 0 \\ \frac{1}{a^2} A_{12} \left(\frac{1}{a} R_1 + \frac{1}{a^2} R_2 A_{21} A_{12} - X_2 \right) \\ I_m \end{bmatrix} \\ S_{ol} P_l &= \begin{bmatrix} \frac{1}{a^2} A_{12} \left(I_m - \frac{1}{a} R_2 \right) B_m \\ 0 \end{bmatrix} \\ K_h S_{oh} &= B_m^{-1} \begin{bmatrix} X_1 + (R_1 + a R_2) A_{12}^{-1} & X_2 - \frac{1}{w_h} R_1 + R_2 \end{bmatrix} \\ T_{ih} &= \frac{1}{w_h} B_m^{-1} (X_2 + R_2) B_m\end{aligned}\quad (16)$$

where $X_2 = 2aI_m + A_{22}$. Besides, for $C_o(sI_n - A_o)^{-1}$,

$$\begin{aligned}S_{ol} &= \frac{1}{a^2} C_m \left(\frac{1}{a} \tilde{R}_2 - I_m \right) A_{21o} A_{12o} C_m^{-1} \\ S_{ol} P_l &= \begin{bmatrix} \frac{1}{a^2} C_m \left(I_m - \frac{1}{a} \tilde{R}_2 \right) A_{21o} & 0 \end{bmatrix} \\ K_h S_{oh} &= \begin{bmatrix} \left[\tilde{X}_1 + A_{21o}^{-1} (\tilde{R}_1 + a \tilde{R}_2) \right] C_m^{-1} \\ \left(\tilde{X}_2 - \frac{1}{w_h} \tilde{R}_1 + \tilde{R}_2 \right) C_m^{-1} \end{bmatrix} \\ T_{ih} &= \begin{bmatrix} 0 & \frac{1}{w_h} \left[\tilde{X}_1 + A_{21o}^{-1} (\tilde{R}_1 + a \tilde{R}_2) \right] \\ 0 & \frac{1}{w_h} (\tilde{X}_2 + \tilde{R}_2) \end{bmatrix}\end{aligned}\quad (17)$$

where $\tilde{X}_1 = a^2 A_{21o}^{-1} + A_{12o}$ and $\tilde{X}_2 = 2aI_m + A_{22o}$.

Proof: First, consider the asymptotic frequency approximations of the sensitivity functions for $(sI_n - A)^{-1}B$. In a

one-*d.o.f.* feedback configuration, $T_o(s) = N(s)\tilde{N}_k(s)$ (see Vidyasagar, 1985) then, the low-frequency asymptotic approximation of $S_o(s) = I_n - T_o(s)$ is $S_{ol} = I_n - N_l\tilde{N}_{kl}$, where $\tilde{N}_{kl} = X_l + R_l\tilde{D}_l$. So, from Lemma A.1 of Appendix, $\Gamma_l = (-1/a^2)A_{21}A_{12}$, X is not a function of frequency and,

$$N_l := \frac{1}{a^2} \begin{bmatrix} cA_{12} \\ 0 \end{bmatrix}, \quad \tilde{D}_l = \begin{bmatrix} 0 & -\frac{1}{a}I_m \\ -\frac{1}{a}A_{21} & -\frac{1}{a^2}A_{21}A_{12} \end{bmatrix} \quad (18)$$

Taking $R_l = [R_1 \ R_2]$, then the result of S_{ol} given by Equation (16) follows. From Appendix, $D_l := (-1/a^2)B_m^{-1}A_{21}A_{12}$, so,

$$P_l = \begin{bmatrix} -A_{21}^{-1}B_m \\ 0 \end{bmatrix} \quad (19)$$

and the result of $S_{ol}P_l$ given by Equation (16) follows. Also, in a one-*d.o.f.* feedback configuration $K_hS_{oh} = \tilde{D}_{kh}^{-1}\tilde{N}_{kh}(I_n - N_h\tilde{N}_{kh}) = \tilde{D}_{kh}^{-1}(I_n - \tilde{N}_{kh}N_h)\tilde{N}_{kh}$, where $\tilde{D}_{kh} = Y_h - R_h\tilde{N}_h$ and $\tilde{N}_{kh} = X_h + R_h\tilde{D}_h$. From Lemma A.1 of Appendix, $\Gamma_h = I_m$, Y is not a function of frequency and,

$$\tilde{D}_h = \begin{bmatrix} A_{12}^{-1} & -\frac{1}{w_h}I_m \\ aA_{12}^{-1} & I_m \end{bmatrix}, \quad \tilde{N}_h = \frac{1}{w_h} \begin{bmatrix} 0 \\ B_m \end{bmatrix} \quad (20)$$

where w_h is a fixed frequency in the high-frequency bandwidth of $P(s)$. Taking $R_h = [R_1 \ R_2]$,

$$\begin{aligned} \tilde{D}_{kh} &= \left(I_m - \frac{1}{w_h}R_2 \right) B_m \quad \text{and} \\ \tilde{N}_{kh} &= \begin{bmatrix} X_1 + (R_1 + aR_2)A_{12}^{-1} & X_2 - \frac{1}{w_h}R_1 + R_2 \end{bmatrix} \end{aligned} \quad (21)$$

Hence, $\tilde{N}_{kh}N_h = (1/w_h)(X_2 + R_2)$ and $\tilde{D}_{kh}^{-1}(I_m - \tilde{N}_{kh}N_h) = B_m^{-1}$ at high frequencies, where $N_h = \begin{bmatrix} 0 \\ (1/w_h)I_m \end{bmatrix}$. So, the result of K_hS_{oh} given by Equation (16) follows. From Equation (20),

$$P_h = \begin{bmatrix} 0 \\ \frac{1}{w_h}B_m \end{bmatrix} \quad (22)$$

and the result of $T_{ih} = K_hS_{oh}P_h$ given by Equation (16) follows. Second, consider the asymptotic frequency approximations of the sensitivity functions for $C_o(s)I_n - A_o)^{-1}$. In a one-*d.o.f.* feedback configuration (see Vidyasagar, 1985), $S_{ol} = D_{kol}\tilde{D}_{ol}$, where $D_{kol} = \tilde{Y}_{ol} - N_{ol}\tilde{R}_l$. So, from Lemma A.2 of Appendix, $\Gamma_{ol} = (-1/a^2)A_{21o}A_{12o}$, \tilde{Y}_o is not a function of frequency and,

$$N_{ol} = \frac{1}{a} \begin{bmatrix} 0 & C_m \end{bmatrix}, \quad \tilde{D}_{ol} = \frac{-1}{a^2}A_{21o}A_{12o}C_m^{-1} \quad (23)$$

Taking $\tilde{R}_l = [\tilde{R}_1^T \ \tilde{R}_2^T]^T$, then the result of S_{ol} given by Equation (17) follows. From Appendix, $\tilde{N}_{ol} = (1/a^2)[A_{21o}$

0], so,

$$P_{ol} = C_m \begin{bmatrix} -A_{12o}^{-1} & 0 \end{bmatrix} \quad (24)$$

and the result of $S_{ol}P_{ol}$ given by Equation (17) follows. Also, in a one-*d.o.f.* feedback configuration $K_hS_{oh} = N_{koh}\tilde{D}_{oh}$, where $N_{koh} = \tilde{X}_o + D_{oh}\tilde{R}_{oh}$. From Lemma A.2 of Appendix, $\Gamma_{oh} = I_m$, \tilde{X}_o is not a function of frequency and,

$$\tilde{D}_{oh} = C_m^{-1}, D_{oh} = \begin{bmatrix} A_{21o}^{-1} & aA_{21o}^{-1} \\ -\frac{1}{w_h}I_m & I_m \end{bmatrix} \quad (25)$$

Taking $\tilde{R}_{oh} = [\tilde{R}_1^T \ \tilde{R}_2^T]^T$, so, the result of K_hS_{oh} given by Equation (17) follows. In a one-parameter configuration $T_{ih} = N_{koh}\tilde{N}_{oh}$ and from Appendix,

$$\tilde{N}_{oh} = \begin{bmatrix} 0 & \frac{1}{w_h}I_m \end{bmatrix} \quad (26)$$

Hence, the result of T_{ih} given by Equation (17) follows. ■

The elements (1, 1) of S_{ol} and $S_{ol}P_l$ into Equation (16) of Lemma 3.1 can be minimized using the control parameters R_2 or a , however, the element (2, 2) of S_{ol} into Equation (16) has a maximum value. For this reason in what follows the velocity entries of the state input reference are set to zero. A solution to the restriction equation $\|G_l\|_\infty = \|G_h\|_\infty$ of Equation (1) into Problem 2.1, when the velocity entries of the state input reference are zero, is proposed by,

Theorem 3.2: Consider the plant $P(s) = H(s)I_n - F)^{-1}G + J \in \mathfrak{R}^{p \times m}$ in the one-parameter observer-controller configuration of Figure 2, under Assumptions A1 to A4 and the change of basis $\chi(t) := T_1x(t)$ and $\eta(t) := T_2x(t)$ where T_1 and T_2 are given by Equations (6) and (7). Let the state input reference be $x_d(t) = [y_d(t) \ 0]^T$, $R(s)$ be $[0 \ r]_m \in \mathfrak{R}\mathcal{H}_\infty^{m \times n}$ and $\tilde{R}(s)$ be $[0 \ r_o]_m^T \in \mathfrak{R}\mathcal{H}_\infty^{m \times n}$, where $r \in \mathfrak{R}$ and $\tilde{r} \in \mathfrak{R}$, and suppose that $K(s)$ and $K_o(s)$ are given by Equation (10) and that A_{21} and A_{21o} are non-singular matrices. Then, the optimal values of r and r_o are,

$$\begin{aligned} r^* &= \frac{a(b_1 - b_3)}{b_2 - b_3 + b_1} \\ r_o^* &= \frac{a(\tilde{b}_1 - \tilde{b}_3)}{\tilde{b}_2 - \tilde{b}_3 + \tilde{b}_1} \end{aligned} \quad (27)$$

where $0 < a \in \mathfrak{R}$,

$$b_1 := \frac{1}{a^2} \|A_{12} [-A_{21} \ B_m]\|_\infty$$

$$b_2 := \left\| B_m^{-1} \begin{bmatrix} 2a^2A_{12}^{-1} + A_{21} & \frac{1}{w_h} (3aI_m + A_{22}) B_m \end{bmatrix} \right\|_\infty$$

$$\begin{aligned}
 b_3 &:= \left\| B_m^{-1} \begin{bmatrix} X_1 & \frac{1}{w_h} X_2 B_m \end{bmatrix} \right\|_{\infty} \\
 \tilde{b}_1 &:= \frac{1}{a^2} \left\| C_m A_{21o} \begin{bmatrix} -A_{12o} C_m^{-1} & I_m \end{bmatrix} \right\|_{\infty} \\
 \tilde{b}_2 &:= \left\| \begin{bmatrix} (2a^2 A_{21o}^{-1} + A_{12o}) \begin{bmatrix} C_m^{-1} & \frac{1}{w_h} I_m \end{bmatrix} \\ (3a I_m + A_{22o}) \begin{bmatrix} C_m^{-1} & \frac{1}{w_h} I_m \end{bmatrix} \end{bmatrix} \right\|_{\infty} \\
 \tilde{b}_3 &:= \left\| \begin{bmatrix} \tilde{X}_1 \begin{bmatrix} C_m^{-1} & \frac{1}{w_h} I_m \end{bmatrix} \\ \tilde{X}_2 \begin{bmatrix} C_m^{-1} & \frac{1}{w_h} I_m \end{bmatrix} \end{bmatrix} \right\|_{\infty} \quad (28)
 \end{aligned}$$

being $X_1 = a^2 A_{12}^{-1} + A_{21}$, $X_2 = 2a I_m + A_{22}$, $\tilde{X}_1 = a^2 A_{21o}^{-1} + A_{12o}$ and $\tilde{X}_2 = 2a I_m + A_{22o}$. Moreover, when r is r^* ,

$$\begin{aligned}
 \|G_l\|_{\infty} &= \|G_h\|_{\infty} \\
 &= \frac{1}{a^2} \left\| \frac{b_2}{b_2 - b_3 + b_1} A_{12} \begin{bmatrix} -A_{21} & B_m \end{bmatrix} \right\|_{\infty} \quad (29)
 \end{aligned}$$

where $G_l := [S_{ol} \ S_{ol} P_l]$, $G_h := [K_h S_{oh} \ T_{ih}]$ and when r_o is r_o^* ,

$$\begin{aligned}
 \|G_l\|_{\infty} &= \|G_h\|_{\infty} \\
 &= \frac{1}{a^2} \left\| \frac{\tilde{b}_2}{\tilde{b}_2 - \tilde{b}_3 + \tilde{b}_1} C_m A_{21o} \begin{bmatrix} -A_{12o} C_m^{-1} & I_m \end{bmatrix} \right\|_{\infty} \quad (30)
 \end{aligned}$$

Proof: First, consider the restriction equation of the sensitivity functions for $(sI_n - A)^{-1}B$. Since $R(s)$ be $[0 \ rI_m]$ and the input reference is $x_d(t) = [y_d^T(t) \ 0]^T$, then only the elements (1, 1) of S_{ol} and $K_h S_{oh}$ that are given by Equation (16) of Lemma 3.1, are considered to minimize the criterion given by Equation (3), that is,

$$\begin{aligned}
 G_l &= \frac{1}{a^2} \left(1 - \frac{r}{a} \right) A_{12} \begin{bmatrix} -A_{21} & B_m \end{bmatrix}, \\
 G_h &= B_m^{-1} \begin{bmatrix} X_1 + ar A_{12}^{-1} & \frac{1}{w_h} (X_2 + r I_m) B_m \end{bmatrix} \quad (31)
 \end{aligned}$$

Hence, when $r = 0$, $b_1 = \|\lim_{r \rightarrow 0} G_l\|_{\infty}$ and $b_3 = \|\lim_{r \rightarrow 0} G_h\|_{\infty}$, and when $r = a$, $b_2 = \|\lim_{r \rightarrow a} G_h\|_{\infty}$. Due to the entries of G_l and G_h are real, their norms behave as straight lines that have an intersection point since $\lim_{r \rightarrow a} G_l = 0$. So, the equation of restriction $\|G_l\|_{\infty} = \|G_h\|_{\infty}$ has a solution in the intersection point of the two straight lines of Figure 3, that is,

$$b_1 - \frac{b_1}{a} r^* = b_3 + \frac{b_2 - b_3}{a} r^* \quad (32)$$

this implies the result of r^* given by Equation (27).

Second, consider the restriction equation of the sensitivity functions for $C_o(sI_n - A_o)^{-1}$. Since $\tilde{R}(s)$ be $[0 \ r_o I_m]^T$,

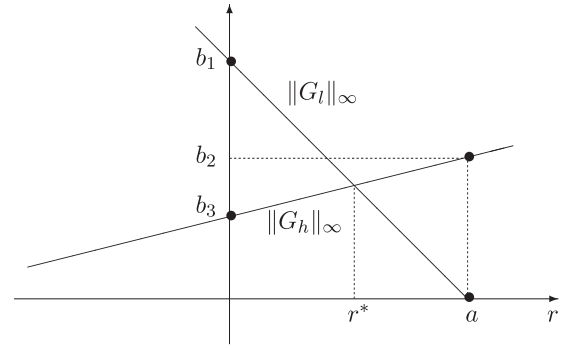


Figure 3. Intersection function for one-d.o.f. feedback configuration.

from Lemma 3.1 and Equation (3),

$$\begin{aligned}
 G_l &= \frac{1}{a^2} \left(1 - \frac{r_o}{a} \right) C_m A_{21o} \begin{bmatrix} -A_{12o} C_m^{-1} & I_m \end{bmatrix}, \\
 G_h &= \begin{bmatrix} (\tilde{X}_1 + ar_o A_{21o}^{-1}) \begin{bmatrix} C_m^{-1} & \frac{1}{w_h} I_m \end{bmatrix} \\ (\tilde{X}_2 + r_o I_m) \begin{bmatrix} C_m^{-1} & \frac{1}{w_h} I_m \end{bmatrix} \end{bmatrix} \quad (33)
 \end{aligned}$$

So, when $r_o = 0$, $\tilde{b}_1 = \|\lim_{r_o \rightarrow 0} G_l\|_{\infty}$ and $\tilde{b}_3 = \|\lim_{r_o \rightarrow 0} G_h\|_{\infty}$, and when $r_o = a$, $\tilde{b}_2 = \|\lim_{r_o \rightarrow a} G_h\|_{\infty}$. The norms of G_l and G_h have an intersection point since $\lim_{r_o \rightarrow a} G_l = 0$. So, the equation of restriction $\|G_l\|_{\infty} = \|G_h\|_{\infty}$ has a solution in the intersection point of the two straight lines of Figure 3, replacing $b_1, b_2, b_3, r, r^*, G_l$ and G_h by $\tilde{b}_1, \tilde{b}_2, \tilde{b}_3, r_o, r_o^*, G_l$ and G_h , respectively. This implies the result of r_o^* given by Equation (27). The results of Equations (29) and (30) follows directly substituting r^* and r_o^* . ■

The solution given by Theorem 3.2 is not unique. Another selection can be done, for instance, $R(s)$ be $[-A_{21} A_{12} - (ar + a^2) I_m \ rI_m] \in \mathfrak{RH}_{\infty}^{m \times n}$ and similarly for $\tilde{R}(s)$. From Lemma 3.1, these elections simplify the terms $X_1 + (R_1 + ar_2) A_{12}^{-1}$ and $\tilde{X}_1 + (\tilde{R}_1 + ar_2) A_{12o}^{-1}$ of the sensitivity functions to zero, that could be desirable for some specific applications.

Remark 3.1: The values of $\|G_l\|_{\infty}$ and $\|G_h\|_{\infty}$ that are given by Equations (29) and (30) of Theorem 3.2 depend mainly on the value of a . These norms are of order $1/a^2$, so, increasing the value of a leads to a solution of Problem 2.1. Also, as the value of a is increased, for a certain value of a the conditions of robust stability of Remark 2.1 are accomplished. However, the location of the closed-loop poles are at $-a$, hence, as the value of a increases, the speed of the output response and the closed-loop low-frequency bandwidth are increased that could amplify $d_m(t)$ and $u(t)$, leading to control saturation. Thus, a compromise exists between these closed-loop requirements and the minimization of criterion (3).

A useful result for the selection of the value of a is,

Corollary 3.3: *Under the assumptions and definitions of Theorem 3.2. If $a^2 \|A_{12}^{-1}\|_\infty \gg \|A_{21}\|_\infty$ and $a^4 \|B_m^{-1} A_{12}^{-1}\|_\infty \gg \|A_{12}[-A_{21} \ B_m]\|_\infty$, then,*

$$a^* \cong \sqrt{\frac{2}{\gamma^*} \|A_{12}[-A_{21} \ B_m]\|_\infty} \quad (34)$$

where γ^* is given by Equation (15).

Proof: If $a^2 \|A_{12}^{-1}\|_\infty \gg \|A_{21}\|_\infty$ then $X_1 \cong a^2 A_{12}^{-1}$ and from Equation (29),

$$\|G_I\|_\infty \cong \left\| \frac{1}{a^2 + \Theta} A_{12}[-A_{21} \ B_m] \right\|_\infty \quad (35)$$

where

$$\Theta := \frac{\|A_{12}[-A_{21} \ B_m]\|_\infty - a^4 \|B_m^{-1} A_{12}^{-1}\|_\infty}{2a^2 \|B_m^{-1} A_{12}^{-1}\|_\infty}.$$

Since $a^4 \|B_m^{-1} A_{12}^{-1}\|_\infty \gg \|A_{12}[-A_{21} \ B_m]\|_\infty$, then,

$$\|G_I\|_\infty \cong \frac{2}{a^2} \|A_{12}[-A_{21} \ B_m]\|_\infty \quad (36)$$

So, the result follows equating this equation to γ^* . ■

The solution of Theorem 3.2 assures strong stability, when $P(s)$ satisfies the *p.i.p.*, as shown by,

Corollary 3.4: *Under the assumptions and definitions of Theorem 3.2, suppose that $P(s)$ satisfies the *p.i.p.*, r be r^* and r_o be r_o^* , where r^* and r_o^* are given by Equation (27). Then, the characteristic polynomials of the stabilizing controllers $K(s)$, $K_r(s)$ and $K_o(s)$ given by Equation (10) are Hurwitz.*

Proof: If $P(s)$ satisfies the *p.i.p.*, then a stable controller exists among the set of all stabilizing controller (see Vidyasagar, 1985). The characteristic polynomials of the stabilizing controllers are,

$$\begin{aligned} \det(\tilde{D}_k(s)) &= \det(Y(s) - R(s)\tilde{N}(s)) \quad \text{and} \\ \det(D_{k_o}(s)) &= \det(\tilde{Y}_o(s) - N_o(s)\tilde{R}(s)) \end{aligned} \quad (37)$$

where $Y(s)$, $\tilde{N}(s)$, $\tilde{Y}_o(s)$ and $N_o(s)$ are given in Appendix, and $R(s) \in \mathfrak{RH}_\infty$ and $\tilde{R}(s) \in \mathfrak{RH}_\infty$ are free control-parameters. From Theorem 3.2, $R(s)$ and $\tilde{R}(s)$ are $[0 \ r/m]$

and $[0 \ r_o/m]$, respectively. So, from Appendix,

$$\begin{aligned} \det(\tilde{D}_k(s)) &= \det\left(\frac{s+a-r}{s+a} B_m\right) \\ &= \det\left(\frac{s+a-r}{s+a} I_m\right) \det(B_m) \quad \text{and} \\ \det(D_{k_o}(s)) &= \det\left(\frac{s+a-r_o}{s+a} C_m\right) \\ &= \det\left(\frac{s+a-r_o}{s+a} I_m\right) \det(C_m) \end{aligned} \quad (38)$$

Since B_m and C_m are non-singular matrices, then the characteristic equations of $K(s)$, $K_r(s)$ and $K_o(s)$ are,

$$\begin{aligned} (s+a-r)^m &= 0 \quad \text{and} \\ (s+a-r_o)^m &= 0 \end{aligned} \quad (39)$$

Since r is r^* and r_o is r_o^* , then the characteristic polynomials of $K(s)$, $K_r(s)$ and $K_o(s)$ are Hurwitz if $a-r^* > 0$ and $a-r_o^* > 0$. Hence, from Equation (27),

$$\begin{aligned} a-r^* &= \frac{ab_2}{b_2-b_3+b_1} \quad \text{and} \\ a-r_o^* &= \frac{\tilde{a}\tilde{b}_2}{\tilde{b}_2-\tilde{b}_3+\tilde{b}_1} \end{aligned} \quad (40)$$

From Theorem 3.2, $a > 0$ is selected and due to the fact that $b_2 > 0$, $b_1 > 0$, $b_2 > b_3$, $\tilde{b}_2 > 0$, $\tilde{b}_1 > 0$ and $\tilde{b}_2 > \tilde{b}_3$, then the result follows. ■

The results are analysed for the reference tracking control problem in the next section and are illustrated by a simulation example of a two cart system in Section 5.

4. Reference tracking control

The one-parameter observer-controller configuration of Figure 2 is replaced by a two-parameter observer-controller configuration as shown in Figure 4. The controller $K_r(s) \in \mathfrak{R}^{m \times p}$ is used to improve the regulation or tracking, and the controller $K(s)$ satisfies closed-loop requirements solving the MSC problem applying Theorem 3.2. In this work $K_r(s)$ is used to solve the reference tracking control problem. If $K_r(s)$ is unstable, it is required to implement into the loop the common coprime denominator of $K(s)$ and $K_r(s)$ (see Vidyasagar, 1985). Using the results of Section 3 the controllers are stable and strong stability is assured if $P(s)$ satisfies the *p.i.p.* (see Corollary 3.4).

In a two-*d.o.f.* feedback configuration $T_o(s) = N(s)Q(s)$ (see Vidyasagar, 1985). Let the input reference be $x_d(t) = [y_d^T(t) \ 0]^T$, so, at low frequencies, from

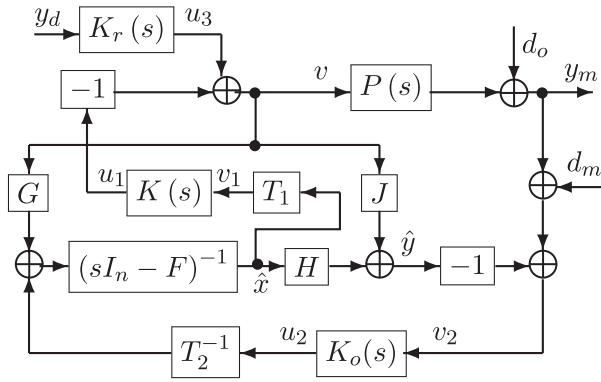


Figure 4. Two-parameter observer-controller configuration.

Equation (18),

$$T_l = \frac{1}{a^2} \begin{bmatrix} A_{12} \\ 0 \end{bmatrix} Q_l \quad (41)$$

The selection,

$$Q_l = a^2 A_{12}^{-1} \in \mathfrak{RH}_{\infty}^{m \times m} \quad (42)$$

solves the reference tracking control problem.

On the other hand, using the lower Linear Fractional Transformation $\mathcal{F}_l(\tilde{P}(s), K(s)) := \tilde{P}_{11}(s) + \tilde{P}_{12}(s)K(s)(I - \tilde{P}_{22}(s)K(s))^{-1}\tilde{P}_{21}(s)$, the criterion (1) can be rewritten as $\min_{K(s)} \|\mathcal{F}_l(\tilde{P}(s), K(s))\|_{\infty}$ where,

$$\begin{aligned} \tilde{P}_{11}(s) &:= \begin{bmatrix} I & P(s) \\ 0 & 0 \end{bmatrix} & \tilde{P}_{12}(s) &:= \begin{bmatrix} -P(s) \\ I \end{bmatrix} \\ \tilde{P}_{21}(s) &:= [I \ P(s)] & \tilde{P}_{22}(s) &:= -P(s) \end{aligned} \quad (43)$$

in the general control scheme of Figure 5 where the transfer function from $d(t) := [d_1^T(t) \ d_2^T(t)]^T$ to $z(t) := [z_1^T(t) \ z_2^T(t)]^T$ is $\mathcal{F}_l(\tilde{P}(s), K(s))$. Using the state space realization of $P(s)$, (F, G, H, J) , a state space description of the generalized plant $\tilde{P}(s)$ is,

$$\begin{aligned} \dot{x}(t) &= Fx(t) + [0 \ G \ -G] \tilde{v}(t) \\ z_1(t) &= Hx(t) + [I \ J \ -J] \tilde{v}(t) \\ z_2(t) &= [0 \ 0 \ I] \tilde{v}(t) \\ y_m(t) &= z_1(t) \end{aligned} \quad (44)$$

where $\tilde{v}(t) := [d_1^T(t) \ d_2^T(t) \ u^T(t)]^T$. This state space description is used into the MatLab function `hinfscyn` selecting γ^* given by Equation (15) as the lower bound of γ and the method based on two Riccati equations. The control objective is that $z_1(t) = y_m(t)$ tracks the input reference $d_2(t) = y_d(t)$ in stationary state. So, a gain Φ is added in the feedback configuration of Figure 5. Let $(F_{cl}, G_{cl}, H_{cl}, J_{cl})$ be the closed-loop state-space description gotten by `hinfscyn` MatLab function, then the closed-loop transfer function at stationary state

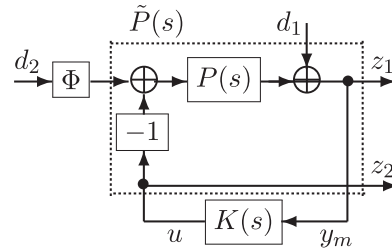


Figure 5. General control scheme for the criterion (1).

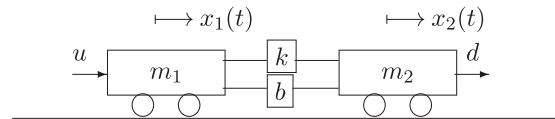


Figure 6. Two cart system.

is $P_{class} = -H_{cl}F_{cl}^{-1}G_{cl} + J_{cl} \in \mathfrak{RH}^{p \times n}$. Let P_{class} be block partitioned as $P_{class} := [P_1 \ P_2]$ where $P_1 \in \mathfrak{RH}^{p \times m}$ and $P_2 \in \mathfrak{RH}^{p \times m}$ and suppose that P_2 is a non-singular matrix. Hence,

$$\Phi = P_2^{-1} \quad (45)$$

In the following section, the results are illustrated by a simulation example of a two cart system.

5. Example of a two cart system

A state-space realization of the two-cart system shown in Figure 6 is,

$$\begin{aligned} F &= \begin{bmatrix} 0 & 0 & 1 & 0 \\ 0 & 0 & 0 & 1 \\ \frac{-k}{m_1} & \frac{k}{m_1} & \frac{-b}{m_1} & \frac{b}{m_1} \\ \frac{k}{m_2} & \frac{-k}{m_2} & \frac{b}{m_2} & \frac{-b}{m_2} \end{bmatrix} & G &= \begin{bmatrix} 0 & 0 \\ 0 & 0 \\ 1 & 0 \\ 0 & 1 \end{bmatrix} \\ H &= \begin{bmatrix} 1 & 0 & 0 & 0 \\ 0 & 1 & 0 & 0 \end{bmatrix} \end{aligned} \quad (46)$$

where $x(t) := [x_1(t) \ x_2(t) \ \dot{x}_1(t) \ \dot{x}_2(t)]^T$ is used as the state, $u(t) = [u_1(t) \ u_2(t)]^T$ is used as the plant input, m_1 and m_2 are the mass, k_1 and k_2 are the stiffness coefficients, and b_1 and b_2 are the friction coefficients.

This system is controllable, observable and satisfies $n = 2m$. Besides, the poles of $H(sI - F)^{-1}G + J$ are $-0.2917 \pm 2.8720i, 0$ and 0 , and does not have transmission zeros, so, $P(s)$ satisfies the *p.i.p.* Notice that G_2 is a nonsingular matrix and using T_1 from Equation (6) keeps the same realization of Equation (46), so, the stabilizing controllers $K(s)$ and $K_r(s)$ of Figures 2 and 4 are obtained from Appendix and Equation (10). Since H_2 is a singular matrix, this system requires the similarity transformation $T_3 = \begin{bmatrix} 0 & I_m \\ I_m & 0 \end{bmatrix}$ before applying T_2 from Equation (7). After

applying T_2T_3 , the stabilizing controller $K_0(s)$ is obtained from Appendix and Equation (10). Simulations were realized on the two-parameter observer-controller configuration of Figure 4 using MatLab-Simulink and considering $k = 10$ N/m, $b = 0.7$ N s/m, $m_1 = 2$ Kg and $m_2 = 3$ Kg, the initial condition $x(0) = 0$ and desired state reference, $x_d = [2 \ 3 \ 0 \ 0]^T$, where the velocity references are set to zero to apply Theorem 3.2.

The solutions of the equations GCARE and GFARE that are given by Equations (14) and (12) are,

$$X_r = \begin{bmatrix} 1.1906 & 0.6199 & 0.8384 & 1.1562 \\ 0.6199 & 2.0371 & 1.1811 & 1.8144 \\ 0.8384 & 1.1811 & 1.8408 & 2.6282 \\ 1.1562 & 1.8144 & 2.6282 & 4.0714 \end{bmatrix} \quad \text{and} \quad (47)$$

$$Z = \begin{bmatrix} 0.4602 & 0.4380 & 0.2018 & 0.2020 \\ 0.4380 & 0.4524 & 0.1977 & 0.1983 \\ 0.2018 & 0.1977 & 0.2903 & 0.1059 \\ 0.2020 & 0.1983 & 0.1059 & 0.2261 \end{bmatrix}$$

respectively. So, from Equations (15) and (34),

$$\gamma^* = 2.6099 \quad \text{and} \quad a^* \cong 2.8366 \quad (48)$$

respectively. A sub-optimal controller is used selecting,

$$\gamma = \gamma^* + 0.01 \quad (49)$$

Let $\text{sys}G$ be the state-space realization of $\tilde{P}(s)$ given by Equation (44), then the state-space realization of the controller K_1 is obtained by the MatLab function,

$$\begin{aligned} & [K_1, CL_1, GAM1, INFO1] \\ & = \text{hinfsyn}(\text{sys}G, m, m', GMAX', \gamma, GMIN', \gamma^*, \\ & \quad 'METHOD', 'ric') \end{aligned} \quad (50)$$

where CL_1 is the closed-loop state-space realization. This controller is implemented on the control scheme of

Table 1. Optimal values for MSC.

$a = 0.75$	$a = 1.8$	$a = a^*$
$r^* = -0.0091$	$r^* = -2.0233$	$r^* = -2.5488$
$r_o^* = 0.3983$	$r_o^* = -1.958$	$r_o^* = -2.015$

Figure 5, where Φ is given by Equation (45), and compared with the stabilizing controller of Appendix where the free control parameters solve MSC and reference tracking control problems in the observer-controller configurations of Figures 2 and 4, respectively.

Selecting $w_h = 300$ and applying Theorem 3.2, Table 1 shows the results of MSC problem for $a = 0.75$, $a = 1.8$ and $a = a^*$ in the intersection of the norms of $\|G_l\|_\infty$ and $\|G_h\|_\infty$ that are given by Equations (29) and (30) of Theorem 3.2.

The free control parameter of $K_r(s)$ is selected from Equation (42).

Figures 7–10 show the results, under additive disturbances $d_m(t) = \sin(300t)$, $t \geq 0$ seg. and $d_o(t) = 1$, $t \geq 22$ seg.. As expected stability is guaranteed and the stabilizing controllers are stable. The outputs track the input references with a very ‘small’ stationary state error when the proposed controller is applied while the outputs of the hinfsyn MatLab function oscillate more at the beginning than the proposed controller. Both controllers require the same amount of energy at stationary state as shown in Figures 9 and 10. Also, according to Remark 3.1, the time response decrease, the closed-loop low-frequency bandwidth increase, and the overshoot of the inputs $u_1(t)$ and $u_2(t)$ is ‘bigger’ as the value of a increase for the proposed controller. Also, the performance is improved due to the solution of the MSC problem, as shown in Figures 7–10. The additive disturbance $d_m(t)$ is attenuated and remains as very ‘small’ oscillations at the outputs in Figures 7 and 8 and more noticeable at

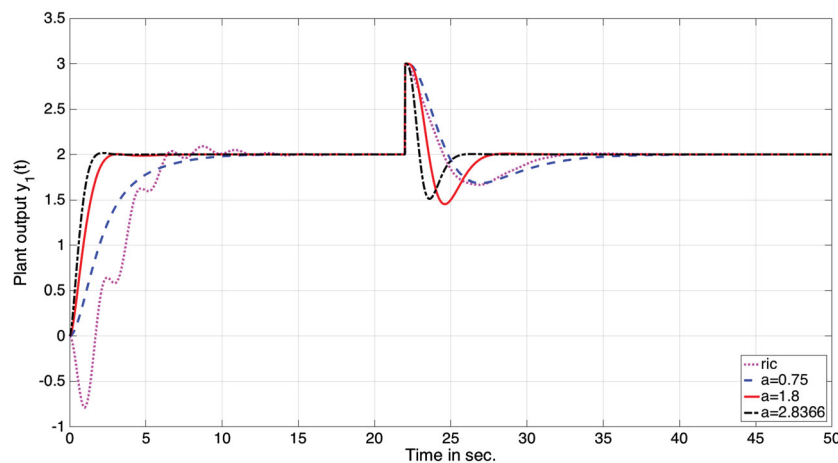


Figure 7. Output $y_1(t)$ applying the MSC controller with the control parameters $a = 0.75$, $a = 1.8$ and $a = a^*$, and compared with the γ -iteration controller based on Riccati (ric) solution.

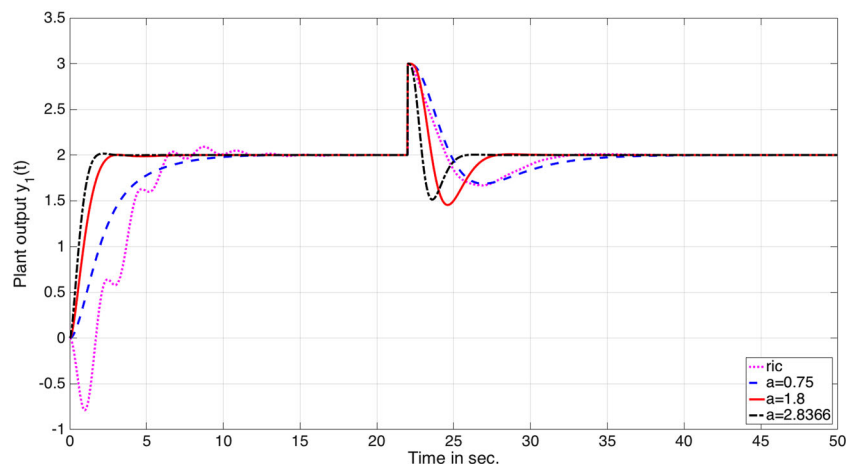


Figure 8. Output $y_2(t)$ applying the MSC controller with the control parameters $a = 0.75$, $a = 1.8$ and $a = a^*$, and compared with the γ -iteration controller based on Riccati (ric) solution.

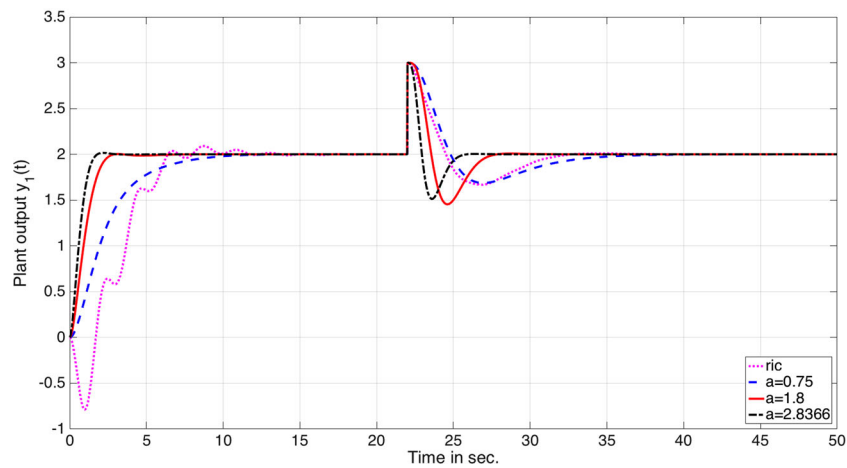


Figure 9. Input $u_1(t)$ applying the MSC controller with the control parameters $a = 0.75$, $a = 1.8$ and $a = a^*$, and compared with the γ -iteration controller based on Riccati (ric) solution.

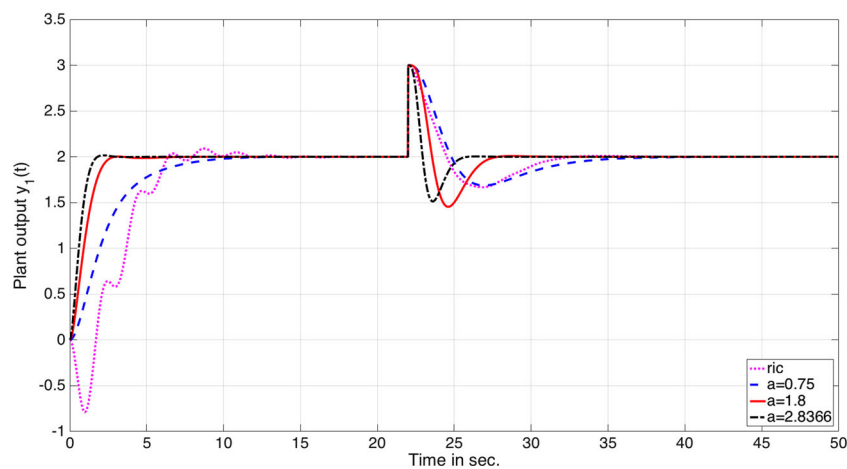


Figure 10. Input $u_2(t)$ applying the MSC controller with the control parameters $a = 0.75$, $a = 1.8$ and $a = a^*$, and compared with the γ -iteration controller based on Riccati (ric) solution.

the control laws in Figures 9 and 10. The amplitude of these oscillations is bigger for the γ -iteration controller. The additive disturbance $d_o(t)$ is attenuated recovering the values at stationary state after a certain time as shown in Figures 7 and 8. As expected the MSC generates smooth trajectories. Since the closed-loop poles are located at $-a$, as the value of a increases the time response decreases and the magnitude of the control input is increased at the beginning of the simulation.

6. Conclusions

A solution to a non-iterative Mixed Sensitivity Control (MSC) problem is proposed. The problem is transformed into an optimization problem without restrictions affine to the free control parameter. The \mathcal{H}_∞ norms of the sensitivity functions in low frequencies are minimized subject to an algebraic equation of restriction that assigns the same value to the \mathcal{H}_∞ norms of the sensitivity functions at low and high frequencies. The results are compared with standard MSC based on γ -iteration and Riccati equations available at MatLab hinfyn function. The results show that the optimal stability margin proposed by Glover and McFarlane (1989) is very useful to tune the proposed stabilizing controllers and the iterative controller. Both control techniques achieve 'good' performance, the trajectories are smooth with 'small' control energy and assure very 'small' stationary state error under additive output and measurement disturbances. Also, the proposed MSC assures stable controllers and low computational effort that is useful for on-line control implementation. The proposed solution can be further used for control problems like linear parametric varying control or fault-tolerant control.

Disclosure statement

No potential conflict of interest was reported by the author(s).

ORCID

R. Galindo Orozco  <http://orcid.org/0000-0002-3402-3644>

References

- Banerjee, A., Ray, N., & Kavasseri, R. (2018). A novel explicit disturbance model-based robust damping of inter-area oscillations through MTDC grids embedded in AC systems. *IEEE Transactions on Power Delivery*, 33(4), 1864–1874. <https://doi.org/10.1109/TPWRD.2018.2799170>
- Cerone, V., Milanese, M., & Regruto, D. (2009). Yaw stability control design through a mixed-sensitivity approach. *IEEE Transactions on Control Systems Technology*, 17(5), 1096–1104. <https://doi.org/10.1109/TCST.2008.2005402>
- Diaz, A., Pujana, A., Ezquerro, J., Milo, A., & Landaluze, J. (2015). Linear models-based LPV modelling and control for wind turbines. *Wind Energy*, 18, 1151–1168. <https://doi.org/10.1002/we.v18.7>
- Doyle, J. C., Glover, K., Khargonekar, P. P., & Francis, B. A. (1989). State-space solutions to standard \mathcal{H}_2 and \mathcal{H}_∞ control problems. *IEEE Transactions on Automatic Control*, 34(8), 831–847. <https://doi.org/10.1109/9.29425>
- Folly, K. (2007). A comparison of two methods for preventing pole-zero cancellation in H_∞ power system controller design. In *IEEE Lausanne power tech*.
- Fomentin, S., & Karimi, A. (2013). A data-driven approach to mixed-sensitivity control with application to an active suspension system. *IEEE Transactions on Industrial Informatics*, 9(4), 2293–2300. <https://doi.org/10.1109/TII.2012.2220556>
- Galindo, R. (2009). Parametrization of all stable controllers stabilizing full state information systems and mixed sensitivity. *Proceedings of the Institution of Mechanical Engineers Part I: Journal of Systems and Control Engineering*, 223(7), 957–971. <https://doi.org/10.1243/09596518JSCE703>
- Galindo, R. (2016). Input/output decoupling of square linear systems by dynamic two-parameters stabilizing control. *Asian Journal of Control*, 18(6), 2310–2316. <https://doi.org/10.1002/asjc.1285>
- Galindo, R., & Conejo, C. (2012). A parametrization of all one parameter stabilizing controllers and a mixed sensitivity problem, for square systems. In International conference on electrical engineering, computing science and automatic control (p. 171–176), Mexico city, Mexico.
- Galindo, R., & Flores, M. A. (2014). LPV control methodology applied to LPV systems based on robust stabilizing controllers and mixed sensitivity. In Congreso latinoamericano de control automatico (p. 1230–1235), Cancún, Quintana Roo, Mexico.
- Glover, K., & McFarlane, D. (1989). Robust stabilization of normalized coprime factor plant descriptions with γ -bounded uncertainty. *IEEE Transactions on Automatic Control*, 34, 821–830. <https://doi.org/10.1109/9.29424>
- Ounis, F., & Golea, N. (2016). PID, 2-DOF PID and mixed sensitivity loop-shaping based robust voltage control of quadratic buck DC-DC converter. *Advances in Electrical and Electronic Engineering*, 14(5), 551–561. <https://doi.org/10.15598/aeae.v14i5.1821>
- Sil, A., Gangopadhyay, T., Paul, S., & Maitra, A. (2009). Design of robust power system stabilizer using H_∞/H_∞ mixed sensitivity technique. In International conference on Power Systems (p. 1–4), Kharagpur, India.
- Sutyasadi, P., & Parnichkun, M. (2016). Gait tracking control of quadruped robot using differential evolution based structure specified mixed sensitivity H_∞/H_∞ robust control. (p. 1–18). Hindawi Publishing Corporation, Journal of Control Science and Engineering, vol. 2016, 1–18, <http://dx.doi.org/10.1155/2016/8760215>.
- Tsai, M., Geddes, E., & Postlethwaite, I. (1992). Pole-zero cancellations and closed-loop properties of an H_∞ mixed sensitivity design problem. *Automatica*, 28(3), 519–530. [https://doi.org/10.1016/0005-1098\(92\)90176-G](https://doi.org/10.1016/0005-1098(92)90176-G)
- Vidyasagar, M. (1985). *Control system synthesis: A factorization approach*. The MIT Press Cambridge.
- Youla, D. C., Bongiorno, J. J., & Lu, C. N. (1974). Single-loop feedback stabilization of linear multivariable dynamical plants. *Automatica*, 10(2), 159–173. [https://doi.org/10.1016/0005-1098\(74\)90021-1](https://doi.org/10.1016/0005-1098(74)90021-1)
- Zhou, K., Doyle, J. C., & Glover, K. (1996). *Robust and optimal control*. Prentice Hall.

Appendix. Analytical solutions of Galindo (2016) and Galindo and Conejo (2012)

l.c.f. and *r.c.f.* of $(sl_n - A)^{-1}B$ and solution of $X(s)N(s) + Y(s)D(s) = I$ are given by,

Lemma A.1: Consider the state space realization given by Equation (2) satisfying assumptions A1 to A5, under the changes of basis T_1 and T_2 given by Equations (6) and (7), in the feedback configuration of Figure 4. Suppose that $A_{12} \in \mathbb{R}^{m \times m}$, $A_{21} \in \mathbb{R}^{m \times m}$ and $B_m \in \mathbb{R}^{m \times m}$ are non-singular matrices, $0 < a \in \mathbb{R}$, then a *l.c.f.* of $(sl_n - A)^{-1}B$ over $\mathbb{R}\mathcal{H}_\infty$ is (see Galindo, 2016),

$$\tilde{D}(s) := \begin{bmatrix} \frac{s}{(s+a)}A_{12}^{-1} & \frac{-1}{(s+a)}I_m \\ a\Gamma(s)A_{12}^{-1} & \Gamma(s) \end{bmatrix}, \tag{A1}$$

$$\tilde{N}(s) := \frac{1}{s+a} \begin{bmatrix} 0 \\ B_m \end{bmatrix}$$

where $\Gamma(s) := (1/(s+a)^2)(s^2I_m - A_{22}s - A_{21}A_{12})$. A *r.c.f.* over $\mathbb{R}\mathcal{H}_\infty$ of $(sl_n - A)^{-1}B$ is (see Galindo & Conejo, 2012),

$$N(s) := \frac{1}{(s+a)^2} \begin{bmatrix} A_{12} \\ sl_m \end{bmatrix}, \quad D(s) := B_m^{-1}\Gamma(s), \tag{A2}$$

where $0 < a \in \mathbb{R}$. Also, in Galindo and Conejo (2012) a solution to $XN(s) + YD(s) = I_m$ over $\mathbb{R}\mathcal{H}_\infty$ is,

$$X := [X_1 \quad X_2] \in \mathbb{R}\mathcal{H}_\infty^{m \times n}, \quad Y := B_m, \tag{A3}$$

where $X_1 := a^2A_{12}^{-1} + A_{21}$ and $X_2 := 2aI_m + A_{22}$.

l.c.f. and *r.c.f.* of $C_o(sl_n - A_o)^{-1}$ and solution of $\tilde{N}_o(s)\tilde{X}_o(s) + \tilde{D}_o(s)\tilde{Y}_o(s) = I$ are given by,

Lemma A.2: Consider the state space realization given by Equation (2) satisfying assumptions A1 to A5, under the changes of basis T_1 and T_2 given by Equations (6) and (7), in the feedback configuration of Figure 4. Suppose that $A_{12} \in \mathbb{R}^{m \times m}$, $A_{21} \in \mathbb{R}^{m \times m}$ and $B_m \in \mathbb{R}^{m \times m}$ are non-singular matrices, $0 < a \in \mathbb{R}$, then a *r.c.f.* of $C_o(sl_n - A_o)^{-1}$ over $\mathbb{R}\mathcal{H}_\infty$ is (see Galindo, 2016),

$$\begin{aligned} N_o(s) &:= \frac{1}{s+a} [0 \quad C_m], \\ D_o(s) &:= \begin{bmatrix} \frac{s}{s+a}A_{21o}^{-1} & aA_{21o}^{-1}\Gamma_o(s) \\ \frac{-1}{s+a}I_m & \Gamma_o(s) \end{bmatrix} \end{aligned} \tag{A4}$$

where $\Gamma_o(s) := (1/(s+a)^2)(s^2I_m - A_{22o}s - A_{21o}A_{12o})$. A *l.c.f.* over $\mathbb{R}\mathcal{H}_\infty$ of $C_o(sl_n - A_o)^{-1}$ is (see Galindo & Conejo, 2012),

$$\tilde{D}_o(s) := \Gamma_o(s)C_m^{-1}, \quad \tilde{N}_o(s) := \frac{1}{(s+a)^2} [A_{21o} \quad sl_m], \tag{A5}$$

where $0 < a \in \mathbb{R}$. Also, in Galindo and Conejo (2012) a solution to $\tilde{N}_o(s)\tilde{X}_o + \tilde{D}_o(s)\tilde{Y}_o = I_m$ over $\mathbb{R}\mathcal{H}_\infty$ is,

$$\tilde{X}_o := \begin{bmatrix} X_{1o} \\ X_{2o} \end{bmatrix} \in \mathbb{R}\mathcal{H}_\infty^{n \times m}, \quad \tilde{Y}_o := C_m \tag{A6}$$

where $X_{1o} := a^2A_{21o}^{-1} + A_{12o}$ and $X_{2o} := 2aI_m + A_{22o}$.